Conf-820741--1

Submitted to the Synchrotron Radiation Conference
Novosibirsk, USSR, July 27-29, 1982

BNL 31571

The National Synchrotron Light Source and Special Radiation-Sources Development*

BNL--31571

DE82 018058

A. van Steenbergen, NSLS Staff
National Synchrotron Light Source, Brookhaven National Laboratory
Upton, NY 11973, U.S.A.

Abstract

Design features are presented of the two high current electron storage rings comprising the National Synchrotron Light Source and its basic parameters are enumerated. In addition, an overview is presented of the special radiation sources under construction and development, including a superconducting wiggler, permanent magnet wiggler, X-ray and VUV undulators, free electron laser source and Compton backscattered γ source.

Introduction

Construction of two storage rings for a multiplicity of high brightness synchrotron radiation sources was recently completed. In addition to present dominant emphasis on commissioning and further upgrading of the two storage rings, construction and developmental efforts are under way to expand the experimental capability, for such diverse fields as the materials sciences, atomic and nuclear physics and biology, by means of a number of special radiation sources based on the wiggler, undulator, free electron laser and Compton backscattered photon concepts.

---

*Work supported by the U.S. Department of Energy.

Facility Design

The injector system for the two storage rings consists of a nominal 70 MeV linear accelerator[1] (S band, $2\pi/3$ mode; 2855 MHz; 1 pulse/sec; 3 accelerating sections; beam current 20 mA; momentum spread, $\Delta p/p = \pm 0.25\%$, beam emittance $\pi\varepsilon = 2\ 10^{-5}$ rad.m.) and a 70-700 MeV booster synchrotron[2] of which the parameters are presented in Table 1. For this synchrotron a hybrid lattice (defocusing gradient "dipole"-focusing quadrupole) has been designed of which the structure is shown in Fig. 1. Notwithstanding the use of combined function elements, the betatron and synchrotron oscillations are damped, an essential feature of the booster, since it will be operated with an adequately long high energy dwell time, in order to achieve minimum beam emittance prior to transfer into either storage ring.

Since both the VUV and X-ray storage rings are designed as dedicated synchrotron radiation sources, their structures are optimized for favorable photon source parameters. This resulted in magnet lattice structures with high magnetic field values, in order to obtain the highest photon energy at minimum rf power requirements. Similarly, higher source brightness is obtained with minimum horizontal emittance. This led in the early designs[3] to the use of achromatic bend sections in the NSLS lattice structures for which the dispersion invariant, $\mathcal{H}$, is minimum, compared with alternate more conventional lattice structures.[4] A favorable consequence of the use of achromatic bend sections is the zero magnitude of the momentum dispersion in the lattice long straight sections, where the rf cavities (reduction of synchrotron-betatron coupling) and wigglers (further reduction of transverse emittance) are located. A superperiod of the X-ray storage ring[5] is shown in Fig. 2. As shown, the achromatic structure is complemented with

quadrupole triplet combinations providing for great flexibility in obtaining a variety of optical solutions. One example of this, the so-called "optics" solution is shown in Fig. 3 indicating the β function and η function behavior in the X-ray lattice. Structure and dynamics of the VUV lattice[6] is similar to that of the X-ray ring. The parameters of both the X-ray ring and the VUV ring are also given in Table I. The VUV lattice and structure functions are given in Fig. 4 and Fig. 5.

The vacuum systems[7] of the storage rings have been designed for an operating pressure of 10^{-9} Torr in order to achieve gas scattering lifetimes in excess of 10 hrs. The vacuum chambers are fabricated from Aluminum extrusions. Two cooling channels are incorporated, as shown in Fig. 6, in order to provide for simple geometries to pass the synchrotron radiation to the external photon lines. This also makes possible a simple crotch design (also shown in Fig. 6) for the synchrotron radiation exit port in the X-ray ring which is subject to perpendicular incidence of the radiation with a high linear power density.

For the magnet system[8] of the storage rings, associated with the objective of providing for ease of synchrotron radiation emergence, C magnets are used for the dipole magnets. All magnets are built up from stamped laminations. These are glued together in elementary blocks of parallelogram cross section, which in turn are assembled into complete units with parallel end faces. End shims, shaped to control the integrated sextupole term, are used.

The NSLS facility is controlled and monitored through a computer network consisting of two Data General ECLIPSE S250 computered connected to 4 Data General NOVA 3/4 computers, each of which in turn is linked via

serial lines to 16 microcomputers.[9] For the external photon lines individual computers will be used ranging from, typically, a limited capability Textronix 4051 system for certain photoelectrospectroscopy lines in the VUV area to a VAX 11/780 system for biological structure research using the X-ray small angle scattering line.

For the acceleration systems a relatively low frequency of 53 MHz has been adopted partly for cost and in-house technology reasons, partly by considering the objective of a minimum over voltage factor in order to minimize the required lattice straight section length for rf structures; the desirability of a low synchrotron oscillation wave number so that potential betatron-synchrotron resonant side bands, which constrain the permissible betatron oscillation frequencies, may be avoided; the desire to reduce heavy beam loading of the rf cavity in order to improve stability of operating conditions (lower shunt impedance guided by reasonable cavity excitation power); and the objective to avoid clearing electrodes in the storage ring vacuum envelope (impedance problem), taking into account that beam neutralization occur for smaller bunch separation.

A single cavity is being used in each storage ring.[10] For the X-ray ring cavity a 0.5 MW drive system[11] will be used by combining four grounded grid tetrode, 125 kW power amplifiers. These units have been individually tested up to 150 kW; consequently with a calculated cavity power dissipation of 150 kW, beam power requirements can be met. For the VUV ring, a similar, but single output stage, 50 kW power amplifier is being used, adequate for the nominal 5 kW cavity power dissipation plus approximately 12 kW beam power requirement.

TABLE 1. NSLS, ACCELERATOR AND STORAGE RING PARAMETERS

	X-RAY STORAGE RING	VUV STORAGE RING	BOOSTER SYNCHROTRON
ENERGY RANGE (GeV)	0.7-2.5	0.7	0.1-0.7
DESIGN CURRENT (A.)	0.5 (1.9 10^{12} e^-)	1.0 (1.1 10^{12} e^-)	0.02 (*10^{10} e^-)
CIRCUMFERENCE (m.)	170.1	51.0	28.35
B(max.), (ρ) (T.), (ω_c)	1.22 (6.875)	1.22 (1.91)	1.22 (1.91)
τ_{ORB} (h) (MSEC)	567.7 (30)	170.2 (9)	94.6 (5)
DAMPING TIMES (SEC.)	$\tau_x=\tau_y$=0.006;τ_ϵ=0.003*	$\tau_x=\tau_y$=0.021; τ_ϵ=0.011	τ_x=0.008; τ_y=0.012; τ_ϵ=0.013
$\tau_{TOUSCHEK}$ (HRS.)	$\geq$8 (2.5 GeV)	$\geq$3**	$\geq$1.4 (0.7 GeV)
LATTICE STRUCTURE	SEP. FUNCT. TRIPLETS, 8f.	SEP. FUNCT. DOUBLETS, 4f.	HYBRID STRUCT., FODO, 4f.
MAGNET COMPLEMENT	16B (2.7 m.)	8B (1.5 m.)	8B (1.5 m.) (+defoc. comp.)
	40Q (0.45 m.), 16Q (0.8 m.)	24Q (0.3 m.)	8Q (0.3 m.) (foc. elem. only)
	32S (0.2 m.)	12S (0.2 m.)	4S (0.2 m.)
NOMINAL TUNES ν_x,ν_y	9.7, 5.7	3.3, 1.3	2.4, 1.4
MOMENTUM COMPACT., α_p	0.0065	0.023	0.106
RF, FREQUENCY (MHz)	52.880	52.880	52.880
RADIATED POWER (KW)	252+35 $H_{WIGGLER}$	11.3	0.22
RF, PEAK VOLTAGE (KV)	800	100	20
DESIGN RF POWER (KW)	500 (300 BEAM)	50	0.4
ν_s	0.0042	0.0022	0.0015
ENERGY SPREAD, (σ_E/E)	8.2 10^{-4}	4.4 10^{-4}	6.4 10^{-4}
BAT. BUNCH, $2\sigma_L$ (cm)	10.5	7.6	16.0
EQUIL. ϵ_x (m.rad)	8.0 10^{-8}	8.8 10^{-8}	4.8 10^{-8}
(K=0.1): ϵ_y (m.rad)	8.0 10^{-10}	8.8 10^{-10}	4.8 10^{-10}

*$\tau_x=\tau_y$=0.26 sec; τ_ϵ=0.13 sec at 0.7 GeV with $\hat{V}_{RF}$=50 kV.

**For $\hat{V}$=100 kV at twice the natural bunch length.

TABLE 2. NSLS SCIENTIFIC UTILIZATION, 1982

	NSLS UV BEAM LINES	λ(Å)		NSLS X-RAY BEAM LINES
U 1.				X 9. A) EXAFS (BIOLOGY) B) SCATTERING
U 2.				
U 3.				
U 4.	A) SEXAFS B) ARUPS C) RELF/MOD. SPECT. D) LITHOG.	12-1200 20-5000 400-6000 WHITE	PGM TGM NIM	X10. A) EXAFS B) X-RAY SPECTROSCOPY X11. EXAFS
U 5.				
U 6.	LITHOGRAPHY	WHITE		
U 7.	A) ARUPS/XPS/SEXAFS B) ARUPS C) INFRARED	15-1200 80-2500 10^4-10^5	PGM TGM NIM	X12. A) SMALL ANGLE SCATTERING B) PROTEIN CRYSTALLOGRAPHY
U 8.	A) ARUPS B) ARUPS B) ARUPS C) EXAFS/SEXAFS/MICR'Y.	18-2000 80-2500 80-2500 8-100	TGM TGM FRESNEL ZONE PLATE	X13. CRYSTALLOGRAPHY/DIFFUSE SCATTERING ENERGY DISPERSIVE DIFFRACTION X14. A) DIFFUSE SCATTERING B) MICROPROBE C) TOPOGRAPHY
U 9.	DICHROISM/FLUORESCENCE FLUORESCENCE LIFETIME	1200-300,000 1050-120,000	NIM NIM	X15. A) SCATTERING X16. B) INTERFEROMETRY
U10.				C) EXAFS/SCATTERING
U11.	GAS PHASE SPECTROSCOPY	300-2000	NIM	D) SPECTROSCOPY
U12.				
U13.				X17. SCATTERING
U14.	A) ARUPS/XPS/SEXAFS B) ARUPS B) ARUPS C) 7M. SPECTROGRAPH	15-1200 80-500 80-500 300-3000	PGM TGM	X18. DIFFRACTION X19. EXAFS/SEXAFS/XPS TOPOGRAPHY X20. A) SCATTERING [LOW Q RESOLUTION] B) SCATTERING [HIGH Q RESOLUTION]
U15.	TGM MONOCHROMATOR	10-80	TGM	X21.
U16.				X22. A) SCATTERING [HIGH Q RESOLUTION] B) SCATTERING [HIGH E RESOLUTION]
				X23. A) TOPOGRAPHY X24. B) SAXS C) EXAFS/SEXAFS D) CRYSTALLOGRAPHY E) XPS/UPS

With regard to experimental utilization the VUV ring has eight 75 mrad ports and eight 90 mrad ports. The X-ray ring provides for (28-N), 50 mrad ports of which each will normally be split in two (or more) branches, subtending typically 10 mrad (or less) of orbit arc per branch, (N is the number of special radiation sources in the X-ray ring, $\hat{N} = 8$). The photon flux versus wavelength spectra for the arc sources are given in Fig. 10, Fig. 13 and Fig. 16. The NSLS facility scientific utilization, status 1982, is given in Table 2.

X-ray Wiggler Sources

Since the critical photon energy (ε_c) is proportional with the B field magnitude (ε_c = Const. BE^2), the critical energy, and with that the available photon flux in the region $\varepsilon > \varepsilon_c$ (arc) can be substantially increased with the use of wiggler magnets. These devices[12,13] perturb the electron orbit locally, typically in a sinusoidal segment trajectory with a maximum local B field of $B_w >> B_{arc}$. In order to extend the photon energy available from the X-ray ring to energies in excess of 100 keV, a high field superconducting wiggler has been designed[14] and is presently in the testing stage. The basic parameters are as follows: 5 poles at 6 T., 2 end poles at 3.9 T., period length, λ_w = 17.42 cm; full gap magnetic 3.2 cm, full gap beam stay clear 2.0 cm; magnetic deflection parameter $K = 0.934\ B_0\lambda_w = 97$. In order to utilize maximum current density in the superconducting NbTi conductor the coil package per pole is made up in two winding layers, as follows: Inner layer, wire 1.06 mm ø, J = 17.3 kA/cm^2, B_c = 8.5 T; outer layer, wire 0.74 mm ø, J = 35.3 kA/cm^2, B_c = 5.7 T. This unit has been tested in a provisional dewar and a

median plane field of 6 T has been achieved. A cross section of the wiggler is shown in Fig. 7 and the photon flux vs. wavelength spectrum is given in Fig. 10 and Fig. 13.

For a specific electron beam energy, the high fields employed in a superconducting wiggler, in order to achieve high ε_c values, have a significant drawback, since the photon source size is enhanced in opening angle proportional to K/γ and the cross sectional magnitude (for small observation angle) proportional to $\lambda_w K/(\pi\gamma)$. This reduces the source brightness and in practical structures limits the available photons to a fraction of the total generated by the wiggler source. With an external acceptance θ_{ext}, the fraction of energy emitted within θ_{ext} is given by

$$P_f = 3.17\ n\ \lambda_w\ E^2\ B_0^2\ I\ (F(\alpha) \qquad \text{with}$$

$$F(\alpha) = (2/\pi)(\alpha + 1/2 \sin 2\alpha) \text{ and} \qquad \sin\alpha = \theta_{1/2,ext}/(K/\gamma)$$

which for the NSLS X-ray superconducting wiggler; with B = 6 T, n = 5 poles, θ_{ext} = 10 mrad; yields $P_{w,tot}$ = 31 kW (end poles neglected) and $P_{f,ext}$ = 9.7 kW. It is obvious, therefore, that if maximum photon energy is not the prime objective, more favorable wiggler structures can be designed with larger number of poles per unit length, smaller radiation opening angle and smaller effective source size. A wiggler design which meets these objectives in a beautiful manner is the Vanadium-Permandur-Rare Earth Cobalt (REC) permanent magnet hybrid wiggler. This device[15], invented by K. Halbach (LBL), emerged from the permanent magnet undulator design[16]. An undulator is a structure consisting of many low field one pole wigglers in sequence with the characteristic that it generates coherent radiation

from the multiplicity of poles.[17] The basic structure of a permanent magnet undulator is shown in Fig. 8. The structure, as shown, is suitable for low field undulators (see below). The field on axis is given by:

B = const. $B_r \exp(-\pi g/\lambda_w) \cdot F(\text{geometry})$, with g = undulator gap, B_r = remanent field, magnet material and $F(\text{geometry}) \simeq 0.5\text{-}0.8$ for various structures. The maximum field is apparently limited by the ratio (g/λ_w) and B_r, a basic permanent magnet material property. It was realized, however, that by cascading the permanent magnet blocks and "guiding" the combined field flux through high μ poles, a much larger on axis field could be obtained without sacrificing magnetic period length. This is illustrated in Fig. 9 where the design principle and engineering execution of an extremely simple, low cost, fixed gap hybrid wiggler structure is shown. The parameters of this wiggler are as follows: 23 poles at 1.5 T (2 end poles at reduced field); λ_w = 13.6 cm; full gap, magnetic, 2.0 cm, full gap beam stay clear 1.8 cm; magnetic deflection parameter $K = 19$, $2\theta_{1/2} = 7.8$ mrad, $2\theta_{1/2,\text{eff}} = 4.6$ mrad ($B \geq 0.8\ B_0$), orbit amplitude deviation (p-p) = 0.16 mm. The photon flux vs wavelength spectrum is shown also in Fig. 10 and Fig. 13. With its λ_c at 2.0Å and 23 full field poles it provides for substantial flux in the wavelength region of 0.5-3Å where the sharp fall off of the arc source spectrum occurs.

Both the superconducting wiggler and hybrid permanent magnet wiggler are in an advanced stage of construction and are expected to be installed within the next year in the X-ray storage ring. In addition to these wiggler sources, because of the experimental interest[18] in a high flux source in the 0.3-1Å region, with minimum opening angle; a superconducting wiggler

design with maximum median plane field values of 3 T is being studied. Tentative parameters are: B = 3T, n = 15 poles, λ_w = 8 cm, K = 22, gap 2 cm.

A distinct drawback of high field wigglers is the large magnitude of total radiation power generated, which creates problems of optical stability in the external photon lines (mirror distortion) and drift in the spectral output of the monochromators. When compared with the superconducting wiggler, the hybrid wiggler total radiation power is substantially less, i.e. 4.4 kW; however, this power is radiated within an opening angle of ≈ 7.8 mrad and the radiation power per unit arc is actually higher than for the superconducting wiggler (see Table 3).

X-ray Undulator Sources

Initially the basic objective in the utilization of an undulator source was the generation of a quasi monochromatic line spectrum given by $\lambda_k = (\lambda_w/2k\gamma^2)(1 + \frac{K^2}{2} + \gamma^2\theta^2)$ and the on axis source brightness enhancement (α N^2, where N is the number of undulator periods).[19-21] Subsequently, the uniqueness of an undulator source used in a high energy electron storage ring was recognized because it provides for a radiation source with extreme collimation, $\theta_{1/2} \approx (1/\gamma)$, and with a high ratio of useful photons per total radiation power generated, as expressed by

$$P_u(k=1) = P_u \left(1 + \frac{K^2}{2}\right)^{-2} \quad \text{with} \quad P_u = 1.9\ 10^{-8}\ N\gamma^2K^2I/\lambda_o$$

where $P_u(k=1)$ is the total power generated in the k=1 mode, and P_u is the total power radiated by the electrons traversing the undulator.

[Alternatively: $dP(w=w_1)/(dw/w) = 3\ P_u\ (1 + \frac{K^2}{2})^{-2}$]

This suggests the use of undulators with very low K values in order to reduce the heating of optical elements by photons outside the spectrum region of interest (say k = 1). However, this tends to limit the available spectrum to higher wavelength values because of the rapid fall off of the spectrum with large undulator mode, k, numbers. Higher photon energy can, of course, be obtained from the undulator by using small magnetic period, λ_w, values. This, however, is limited because of the exponential dependence of B_0 on (g/λ_w) and the undulator structure minimum gap value is limited by specific requirements of storage ring design; such as minimum gap value associated with the magnitude of the beam quantum lifetime ($(g/2) > 8\ \sigma_y$), beam life time associated with rest gas scattering ($1/\tau \sim \gamma^{-2}g^{-2}$) and enhancement of the growth rate for the transverse resistive wall instability ($1/\tau \sim \beta_0\ g^{-3}$). (For the NSLS storage ring these considerations suggest a minimum gap: X-ray, $g \geq 8$ mm; VUV, $g \geq 14$ mm. In effect, therefore, the highest photon energy available, with suitable choice of the undulator K value, is set by the minimum gap the storage ring tolerates, without deleteriously affecting normally achievable beam intensity. Having adopted a minimum gap value, the choice of undulator parameters is narrowly guided by the desired spectrum range, radiation opening angle, heating of optical elements and desire for optimum source brightness. With the above considerations taken into account, the parameters for a high energy undulator, $2<\lambda < 12$Å (HEU) and for a soft X-ray undulator $6 < \lambda < 60$Å (SXU) have been developed and preliminary design studies have been carried out. The parameters for these units are tablulated in Table 3

and the undulator spectra are given in Fig. 11. In this figure the spectral structure of the HEU undulator is shown in detail. For the SXU undulator the mean photon flux versus wavelength is given, since for higher K values (and integrating over all radiation angles) the line spectrum aspects of the undulator is strongly reduced. This is also shown in Fig. 12 where the true spectral structure is given for the SXU undulator. It is evident that for the undulators the ratio (N_{max}/N_{min}) vs λ approaches unity for higher undulator K values. This can be expressed as follows: For $K \gg 1$, the value of k_c is given by $(3/8)K^3$, where k_c is the harmonic number of the critical frequency ($w_c = k_c w_1$). Since at w_c many undulator harmonics, k, contribute the magnitude of $(N_{max}-N_{min})/N \; \alpha(1/k_c)$ or $\alpha \; K^{-3}$.

Intercomparing the spectra and parameters of these two undulators it shows, that the spectral coverage of the HEU, K = 1.4 and the SXU, K = 3 is quite similar in the 2-12Å region. The total undulator radiated power is similar ($\alpha \; NK^2/\lambda_w$), for fixed total undulator length, but the opening angle of radiation is a factor of two less for the HEU unit. In this case, however, the HEU undulator must operate with a gap value as low as 11 mm in the X-ray storage ring, which may not be possible. Accepting, however, an order of magnitude less flux from the HEU unit above 2-3 keV, and the strong line spectrum nature, as compared with the SXU unit; when set, with an acceptable gap value at approximately 20 mm, at K = 0.5, it provides for an extreme collimated ($2\theta_{1/2} \simeq 1/\gamma \simeq 0.2$ mrad), lower total power (reduced by an order of magnitude), high brightness (see below) undulator source in the spectral region (tunable) around ~2 keV (~6Å).

Table 3. UNDULATOR PARAMETERS (X-RAY)

	HEU	SXU
STRUCTURE	VP-SmCo$_5$ HYBRID	
NUMBER OF PERIODS	80	40
PERIOD LENGTH λ_w	3.0 cm	6.0 cm
FULL GAP (MAGN. + STAY CLEAR)	5-25 mm, VARIABLE	
FULL GAP, OPERATIONAL OBJECTIVE	10 mm	
UNDULATOR LENGTH	2.5 m	
DEFLECTION PARAMETER	1.7-0.6	5.0-3.0
GAP	10-20	10-20
$2A\dot{\theta}_x$	0.7-0.25 mrad	2.0-1.2 mrad

X-ray Source Comparison

The theoretical performance parameters of the various special radiation sources for the X-ray ring, as mentioned above, have been evaluated in terms of photon flux,[22,23] central "brightness" at the critical frequency $[d\dot{N}/d\emptyset d\Psi(dw/w)]_{\Psi=0,w=w_c} = B_{\Psi=0}(w=w_c)$; and average source brightness[24] at the critical frequency,

$[d\dot{N}/\text{unit area source/unit solid angle/}(dw/w)] = \langle B\rangle_{w=w_c}$

and have been compared with the X-ray arc source parameters. Relevant expressions for this have been gathered and are listed in the Appendix. Associated with the inherent length of the wigglers and undulators the "depth of field" broadening[25] of the sources have been taken into account by using appropriate expressions for the effective source cross section and radiation angles. The results of this evaluation are given in Table 4. The results are, in general, self-explanatory, indicating now quantitatively for realizable wigglers and undulators the significant flux and brightness enhancement achievable when compared with an X-ray arc source. The $\langle SB\rangle_{w=w_c}$ for the wigglers have been calculated taking instead of the total radiation angle available, (K/γ), a more realistic fraction of

TABLE 4. NSLS SPECIAL RADIATION SOURCES (E = 2.5 GeV, I = 0.5A)

Source	B	ε_c	$(dP/d\phi)_{MAX}$	[1]$F_o(\alpha)$	Flux ($\times 10^{14}$)	[2]B_o ($\times 10^{14}$)	[3]$\langle SB \rangle$ ($\times 10^{15}$)
	kG	keV	W/mrad		Ph/s/mrad/1%$\frac{d\omega}{\omega}$ at $\lambda=\lambda_c$, all Ψ	Ph/s/mrad^2/1%$\frac{d\omega}{\omega}$ at $\lambda=\lambda_c$, $\Psi=0$	Ph/s/mrad^2/mm^2/1%$\frac{d\omega}{\omega}$ at $\lambda=\lambda_c$
(ARC	12.2	5.1	40.1	--	2	3	2)
LHW	15.0	6.2	1198	16.5%	48	74	[5] 4.5
SUW1	60.0	24.9	998	3.2%	10	[4] 15/2	[5] 9.3
SUW2	30.0	12.5	1490	14.1%	30	46	[5] 14

	$2\theta_{1/2}$	ε_1	P_w	(P_{w1}/P_w)	$F_o(\alpha)$	Flux ($\times 10^{14}$)$_{\omega_1}$	B_o ($\times 10^{14}$)$_{\omega_1}$	$\langle SB \rangle$ ($\times 10^{15}$)$_{\omega_1}$
	mrad	keV	kW			Ph/s/1%$\frac{d\omega}{\omega}$	Ph/s/mrad^2/1%$\frac{d\omega}{\omega}$	Ph/s/mrad^2/mm^2/1%$\frac{d\omega}{\omega}$
HEU	0.57	1.0	1.2	0.26	100%	570	1400	260
SXU	1.2	0.18	1.4	0.03	91%	470	150	28

[1] $F_o(\alpha)$ = fraction of total wiggler/undulator radiated power in (within) 1 mrad, at $\theta_{OBS} = 0$.
[2],[3] Definition, see text. [4] Observation centered on $X = \pm K\lambda_0/2\pi\gamma$. [5] $\theta_{x,EXT} \leq 5$ mrad.

the radiation flux within an external acceptance angle of $\theta_{1/2,ext} = 5$ mrad. Also, for the case of the high field wigglers transverse source splitting will occur since $(\lambda_0/2\pi)(K/\gamma)$, the electron orbit maximum deflection in the wiggler, is $>>\sigma_x$, resulting thereby in two distinct domains of high photon density in the photon source phase space distribution. In the central "brightness" magnitude for the SUW1 source, as listed, this is approximated by dividing the peak brightness value by a factor of two. The advantages of the undulators as special radiation sources is evident from these results, both in terms of flux, on axis "brightness" and average brightness. Although the total flux available (at $w=w_1$) for the HEU and SXU undulators are similar, the source brightness values are an order of magnitude larger for the HEU undulator, when compared with the SXU undulator.

Taking specifically also spectral coverage into account, an alternative comparison of the various X-ray sources has been made by assuming an experimental beam line horizontal acceptance angle of 5 mrad and comparing $\dot{dN}/(\frac{dw}{w})$ vs wavelength for the arc, wigglers and the SXU source. This is shown in Fig. 13. Both the results listed in Table 4 and in Fig. 13 indicate the desirability of having a variety of sources available, as listed, in order to meet various experimental demands.

VUV Undulator Sources

The VUV ring permits inclusion of two special sources in its magnetic lattice structure. One of the straight sections will be used for a Free Electron Laser experiment and is expected to evolve as a special FEL source for experimental usage. The undulator for this experiment,

presently in final stages of assembly, can, however, also be used as a generator of "natural" undulator radiation. The parameters of this undulator are as follows: Permanent magnet ($SmCo_5$) structure, N = 38, λ_w = 6.5 cm, variable gap 1-6 cm, deflection parameter K = 4.3-0.4; for g = 2.0 cm, K = 2.4, $2\theta_{1/2}$ = 3.5 mrad. A cross section of the undulator is shown in Fig. 14. Its spectrum, at E_e = 0.7 GeV, is given in Fig. 15 for K = 1, integrated over all Ψ angles but for fractional horizontal acceptance, $\gamma\theta$ = K/2. Alternatively, its spectrum, for K = 2.4, integrated over all angles, is essentially identical to that shown in Fig. 12 for the X-ray ring, except that its wavelength scale is shifted by a factor of approximately 10 towards larger wavelength. For the latter case, compared with the regular VUV arc source, as shown in Fig. 16, when used in a mode of 10 mrad external acceptance, the undulator provides for a factor of 400 flux enhancement in the 200-2000Å spectral region. In terms of source brightness the undulator parameters are summarized in Table 5, where the same notation is valid as used in Table 4 and the Appendix.

Although it is planned to use the VP-REC hybrid wiggler in the X-ray ring, its spectral output when placed in the 0.7 GeV VUV ring is of interest when compared with the VUV arc source. This is also shown in Fig. 16. Compared both with the undulator and the arc source it provides for substantial flux enhancement in the spectral region of 20-100Å where high throughput monochromators are difficult to achieve.[26] If the spectral region above 200Å is of experimental interest, the undulator provides for a more favorable source both in terms of source brightness and lower total radiation power output (factor of 10) when compared with the hybrid wiggler.

TABLE 5. NSLS SPECIAL RADIATION SOURCES (E = 0.7 GeV; I = 1A)

	$2\theta_{1/2}$ mrad	ϵ_1 eV	P_u kW	(P_{u1}/P_u)	F (a)	Flux $(\times 10^{14})_{\omega_1}$ Ph/s/ 1% $\frac{d\omega}{\omega}$	$B_\omega(\times 10^{14})_{\omega_1}$ Ph/s/mrad^2/1% $\frac{d\omega}{\omega}$	$\langle S\Sigma\rangle(\times 10^{15})_{\omega_1}$ Ph/s/mrad^2/mm^2/1% $\frac{d\omega}{\omega}$
FEL U.	3.5	18 (6-60)	0.12	0.07	37%	806	309	4.6

The Free Electron Laser Source

In the course of developmental work at the NSLS towards brighter and higher flux radiation sources in association with the NSLS electron storage rings, it was realized that combining the Free Electron Laser concept with the unique properties of the high current stored electron beam in the UV ring, i.e., low beam emittance, small beam energy spread and large peak current, could lead to a very high brightness, high flux, special radiation source in the 2000-4000Å region.[27] While the operation of a FEL with single passage of electrons has been verified experimentally[28] only limited experimental results are available of a circulating beam driven FEL. Consequently, a proof of principal experiment was proposed and is presently being carried out.[29] The experiment will be done in two phases, i.e. the amplifier experiment and the oscillator experiment. In the amplifier mode the laser beam from an external argon ion laser will be directed through the electron beam undulator interaction region and the single pass gain will be measured. Subsequently, the optical cavity will be completed by means of end mirrors and the laser oscillating mode will be established. The experimental arrangement is shown in Fig. 17. Principally, in the free electron laser, the circulating electron beam of the storage ring exchanges energy with the laser radiation field in the presence of an undulator in which the electrons execute transverse oscillations. With the laser beam

propagating coaxially with the electron beam, the oscillating transverse electric field of the laser can exchange energy with the transverse oscillating electrons provided that the laser field is phased correctly relative to the electron oscillations. The resonance condition is given by $\lambda = \lambda_u(1 + K^2/2)/(2\gamma_r^2)$ with $\gamma_e = \gamma_r$, i.e. the condition for energy transfer is that the radiation wavelength is close (but not equal) to that of the wavelength of "natural" undulator radiation. The electromagnetic field energy gain per pass through the undulator interaction region, within specific limits of electron beam energy spread and angular divergence, is given by:

$$G = (\Delta\varepsilon^2/\varepsilon^2) = 4.5\ \pi^2\gamma_r\lambda^2 N_u^3 k^2 (1+k^2)^{-2} (I_p/I_A)\Sigma_{h\nu}^{-1}$$

with $k = (K_u/\sqrt{2})$, I_p = peak electron current, $I_A = 17.10^3$A, and $\Sigma_{h\nu} = \Sigma_e$, the electron or photon beam cross section. The laser field energy increases exponentially as exp(Gn), where n is the number of traversals, as a consequence of the progressive increasing electron beam energy spread. Net zero gain occurs when the electron beam energy spread is given by $(\Delta E/E) \sim 1/(2N_u)$. The increase of $(\Delta E/E)$ is counterbalanced by the synchrotron radiation damping, leading to a steady state condition whereby the laser power is given by $P \simeq U_o I_o/2N_u$ where U_o is the total synchrotron radiation power radiated.[30] The line width of the laser radiation is given by $(\Delta w/w) = \lambda/\sigma_{//}$ where $\sigma_{//}$ is the electron bunch length.

The FEL experimental parameters are given in Table 6. Taking λ = 3000Å, $\sigma_{//}$ = 6 cm, U_0 = 3 keV, $\langle I \rangle$ = 1A, η = 1%, results in $(\Delta w/w) \simeq 5\ 10^{-6}$, $P_{ext} \simeq 10$ W.

In terms of photon flux and source brightness the relevant quantities are given in Table 7, together with the corresponding values for the FEL undulator as a "natural" undulator source. The uniqueness of the FEL as a special radiation source is evident from this comparison. Compared with, in present terms, a high brightness undulator source, its flux spectral density is six orders of magnitude higher and its source brightness value six to seven orders of magnitude higher. In addition, its line width $(\Delta w/w) \approx 5\ 10^{-6}$, truly a monochromatic source when compared, typically, with the undulator natural radiation first order line ($\Delta w/w \approx 1/N \approx 10^{-2}$).

The present FEL development focuses on the 2500-4500Å region, partly set by storage ring parameters, partly by the reflectivity fall off of the FEL cavity mirrors below 2500Å. Eventually, it is planned to extend development into the spectral region below 2500Å.

TABLE 6. FEL EXPERIMENTAL PARAMETERS

e^- STORAGE RING:		LASER CAVITY:	
ENERGY	300-500 MeV	L_c	17.0 m
INTENSITY	1A, AVERAGE, 3 BUNCHES	CAVITY LOSS, 3510 Å	2%
U_0/TURN	0.4-3.2 keV	WAIST, w_0	0.37 mm
UNDULATOR:		FEL EXPECTED PERFORMANCE:	
FIELDS	PERMANENT MAGNETS	λ	2500-4500 Å
$\hat{B}$	0.1-0.7 TESLA	G_0 (SMALL SIGNAL GAIN PER PASS)	6-18%
PERIOD	λ_u=6.5 cm, N=38	OSCILLATOR POWER	5-15 W
GAP	1-6 cm	LINE WIDTH, $\Delta w/w$	10^{-6}

TABLE 7. NSLS SPECIAL RADIATION SOURCES, FEL VS UNDULATOR

	$2\theta_{1/2}$ mrad	ε eV	P W	Flux Ph/s/$10^{-3}\frac{d\omega}{\omega}$	B_o Ph/s/(0.1 mr)^2/$10^{-3}\frac{d\omega}{\omega}$	<SB> Ph/s/(0.1mr)^{2}mm^2/$10^{-3}\frac{d\omega}{\omega}$
UNDULATOR (FEL)	3.5	18	120	$8\ 10^{12}$	$3\ 10^{10}$	$5\ 10^{9}$
FEL SOURCE	0.3	6.2	10	$3\ 10^{18}$	$3\ 10^{16}$	$7\ 10^{16}$

Compton Photon Source

In the development of the structure for the FEL experiment it became evident that by suitable displacement of the lasing cavity head-on encounters could be produced between the oscillating FEL photon bunches and the circulating electron bunches in the VUV ring, resulting in hard γ radiation as a result of the Compton backscattering. Depending on the FEL wavelength, or, when using an external laser, the laser wavelength, γ energies of up to 30 MeV could be made available. This stimulated the development of a higher energy γ source, by combining an external laser with the X-ray ring, of greater interest to a possible medium energy nuclear physics program.[31] From kinematical considerations of the photon-electron head-on collision[32] the various quantities of interest, i.e., backscattered photon energy, resolution, flux and polarization can be derived. The relevant equations are summarized in Table 8. Assuming now either the use of an external Argon ion laser or the use of the radiation from the VUV ring FEL source[33], γ radiation of up to 500 MeV can be generated. This is shown in Fig. 18. Energy resolution would be enhanced by means of scattered electron momentum determination ("tagging"). The presently developed experimental arrangement plus set of e^- beam, external laser source and

resulting γ beam parameters[33] are given in Fig. 19. Evidently this highly polarized, monochromatic, low background, hard photon source would constitute a unique source for photon nuclear physics.

TABLE 8. COMPTON BACKSCATTERED γ SOURCE

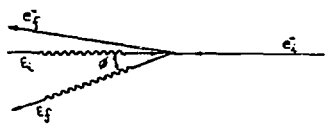

ENERGY: $\varepsilon_f' = 4\gamma^2\varepsilon_i' / (1 + 4\gamma\varepsilon_i' + \theta^2\gamma^2)$

WITH $E_\gamma = \varepsilon_f' \ (m_e c^2)$; $\varepsilon_i = \varepsilon_i'(m_e c^2) = h\nu_L = \varepsilon_{Laser}$

RESOLUTION: $(\Delta\varepsilon_f / \varepsilon_f) = \gamma^2\theta^2 / (1 + 4\gamma\varepsilon_i' + \theta^2\gamma^2)$ $\theta = \theta_c^2 + \theta_e^2$

WITH θ_c = COLLIMATION ANGLE ; θ_e = ELECTRON BEAM DIVERGENCE

FLUX: $I_\gamma = 2\int_{\Delta\Omega}\left(\frac{d\sigma}{d\Omega}\right) L_{sc}\, d\Omega$; $L_{sc} = N_e N_{\varepsilon_i} \int_{path} n_b / \Sigma$

WITH $N_e = \langle I_e \rangle (\pi R)/ec$; $N_{\varepsilon_i} = P_{Laser} L_{int} / \varepsilon_i c$

AND $\frac{d\sigma}{d\Omega} = \left(\frac{r_0}{2}\frac{\varepsilon_f'}{\varepsilon_i'}\right)^2 \left[1 + \frac{2\varepsilon_i'\varepsilon_f'}{(1+\theta^2\gamma^2)} - \frac{2\theta^2\gamma^2}{(1+\theta^2\gamma^2)^2}\right]$

POLARIZATION: $P(\theta) \simeq 1 - \Delta\varepsilon_f / \hat{\varepsilon}_f\,|^2 \approx 1 - (\gamma\theta)^4$ for $\theta \ll 10^{-4}$ r.

Summary

The special radiation sources, in construction and under development at the National Synchrotron Light Source are summarized in Table 9. The special source distribution, both in the X-ray and UV ring are given in Fig. 20. The addition of these special high flux, high brightness, sources to the basic NSLS arc sources will provide for a unique experimental capability which should open up new pathways in experimental techniques in such areas as condensed matter physics, spectroscopy of atoms, dynamic spectroscopy, etc.

TABLE 9. SPECIAL RADIATION SOURCES, NSLS

SHW - SHORT HYBRID WIGGLER, λ_c = 2.0A, 12 POLES
1 - 100A AND ABOVE (10 - 0.1 keV AND BELOW)

$h\nu$-e^- - PHOTON - ELECTRON COLLISION REGION FOR GENERATION OF HARD COMPTON PHOTONS (UP TO 300 MeV)

HEU - HIGH ENERGY UNDULATOR FOR GENERATION OF EXTREME COLLIMATED PHOTON BEAMS (~0.4 mrad): 2 - 12A (6 - 1 KeV)

SUW - SUPERCONDUCTING WIGGLER; λ_0 = 0.174 m, K = 97, λ_c = 0.5A; 5P.6T. + 2P.3T., 0.1 - 10A AND ABOVE (100 - 1 keV AND BELOW)

LHW - LONG HYBRID WIGGLER; λ_0 = 0.136 m, K = 19, λ_c = 2.0A, 24 POLES
1 - 100A AND ABOVE (10 - 0.1 keV AND BELOW)

SXU - SOFT X-RAY UNDULATOR FOR GENERATION OF EXTREME COLLIMATED PHOTON BEAMS (~1.0 mrad); 6 - 60A (2 - 0.2 KeV)

FEL - FREE ELECTRON LASER SOURCE, 2500 - 4500A
ALTERNATIVE: UNDULATOR RADIATION SOURCE 100-2000A.
UNDULATOR; λ_0 = 0.065, K = 2.4 - 0.4, ε_1 = 7 - 66 eV, N = 38

UVU - ULTRA VIOLET UNDULATOR FOR GENERATION OF EXTREME COLLIMATED PHOTON BEAMS IN THE 100-1000A SPECTRAL REGION

(SUW2 - SUPERCONDUCTING WIGGLER, λ_c = 1A; 15 POLES, λ_0 = 0.08 m, K = 22)

IN CONSTRUCTION

APPENDIX: FLUX, CENTRAL SPECTRAL "BRIGHTNESS" AND AVERAGE SPECTRAL BRIGHTNESS EXPRESSIONS FOR MAGNET ARC, WIGGLER AND UNDULATOR SOURCES

ARC SOURCE, FLUX: $\dot{dN}(\omega=\omega_c) = 0.18\ d\gamma\,(I/e)\frac{d\omega}{\omega}$ [PH/S/MRAD/$\frac{d\omega}{\omega}$]

CENTRAL "BRIGHTNESS": $B_{\gamma=0}(\omega=\omega_c) = 4\pi\ 10^{-5}\ \frac{\gamma}{e\epsilon_c}\left(\frac{dP}{d\phi}\right)\frac{d\omega}{\omega}$ [PH/S/MRAD^2/$\frac{d\omega}{\omega}$]

AVERAGE BRIGHTNESS[15]: $\langle SB\rangle_{\omega=\omega_c} = (\dot{dN})/((2.4)^3\ \sigma_x\cdot\sigma_z(\frac{\phi_z}{2}))$ [PH/S/MRAD^2/MM^2/$\frac{d\omega}{\omega}$]

WITH $(\frac{\phi_z}{2}) = (1/\gamma^2 + \sigma_z^2,)^{1/2}$

WIGGLER SOURCE, SINUSOIDAL FIELD, POLES n, LENGTH $\frac{n\lambda_0}{2}$, EXTERNAL ACCEPTANCE θ_{EXT}

FRACTION OF ENERGY EMITTED WITHIN θ_{EXT}: $P_f = 3.17\ n\ \lambda_0\ E^2 B_0^2 I F(d)$ WITH

$F(d) = (2/\pi)(d + \frac{1}{2}\sin 2d)$ AND $\sin d = \theta_{\frac{1}{2},EXT}/2(K/\gamma)$; $\theta_{EXT.} = 1$ MRAD; $[\frac{dP}{d\phi}]_b = P_F(d=d_0)$

FLUX: $\dot{dN}_W(\omega=\omega_c) = \frac{0.404}{\epsilon_c e}\left[\frac{dP}{d\phi}\right]_0\frac{d\omega}{\omega}$ [PH/S./MRAD/$\frac{d\omega}{\omega}$]

CENTRAL "BRIGHTNESS": $B_{0,W}(\omega=\omega_c) = 4\pi 10^{-5}\ \frac{\gamma}{e\epsilon_c}\left[\frac{dP}{d\phi}\right]_0\frac{d\omega}{\omega}$ [PH/S/MRAD^2/$\frac{d\omega}{\omega}$]

AVERAGE BRIGHTNESS: $\langle SB\rangle_{0,W}(\omega=\omega_c) = (\dot{dN}_W)/((2.4)\ \sigma_{x,eff}\ \sigma_{z,eff}(\phi_z/2))$ [PH/S/MRAD^2/MM^2/$\frac{d\omega}{\omega}$]

WITH $2\sigma_{X,EFF} = \left(\frac{n\lambda_0\phi_x}{4} + 2\sigma_x\right)$; $\phi_x = 2(1/\gamma^2 + \sigma_x^2,)^{1/2} + \theta_{\frac{1}{2},ext.}$

AND $2\sigma_{Z,EFF} = \left(\frac{n\lambda_0}{4}\phi_z + 2\sigma_z\right)$; $\phi_z = 2(1/\gamma^2 + \sigma_z^2,)^{1/2}$

UNDULATOR SOURCE, SINUSOIDAL FIELD, N PERIODS, LENGTH $N\lambda_0$

FLUX: $\dot{dN}(\omega=\omega_1) = \frac{\pi\alpha}{e}\frac{NIK^2}{(1+\frac{K^2}{2})}\frac{d\omega}{\omega}$ [PH/S/$\frac{d\omega}{\omega}$] ; $\omega_1 = \frac{2\pi c}{\lambda_0}\frac{2\gamma^2}{(1+\frac{K^2}{2})}$

CENTRAL "BRIGHTNESS": $B_{0,U} = 4.56\ 10^8\ N^2 I\gamma^2 F_1(K)$ [PH/S/MRAD^2/$\frac{d\omega}{\omega}$]

AVERAGE BRIGHTNESS: $\langle SB\rangle_{0,U} = B_{0,U}/((2.4)^2\sigma_{X,EFF}\sigma_{Z,EFF})$ [PH/S/MRAD^2/MM^2/$\frac{d\omega}{\omega}$]

WITH $\sigma_{X,EFF}, \sigma_{Y,EFF}$ AS ABOVE, USING $N = \frac{n}{2}$ AND $\theta_{\frac{1}{2},EXT} = (K/\gamma)$

REFERENCES

1. K. Batchelor, J. Bittner, T. Dickinson, V. Racaniello, J. Sheehan, "The Linac for the National Synchrotron Light Source", BNL Inf. Rep. BNL-26962.

2. J. Galayda, L. Blumberg, R. Heese, J. Schuchman, S. Krinsky, A. van Steenbergen, "The NSLS Booster Synchrotron," IEEE Trans. Nucl. Sci. NS-26, 3839 (1979).

3. R. Chasman, G.K. Green, Nat'l. Conf. Part. Accel., Dubna, USSR, 1976. (BNL 21849).

4. A. van Steenbergen, "Optimization of a Synchrotron Radiation Source," Nucl. Instr. & Methods 177, No. 1, 53 (1980).

5. S. Krinsky, L. Blumberg, J. Bittner, J. Galayda, R. Heese, J. Schuchman, A. van Steenbergen, "Design Status of the 2.5 GeV National Synchrotron Light Source X-ray Ring," IEEE Trans. Nucl. Sci. NS-26, 3806 (1979).

6. L. Blumberg, J. Bittner, J. Galayda, R. Heese, S. Krinsky, J. Schuchman, A. van Steenbergen, "National Synchrotron Light Sourve VUV Storage Ring," IEEE Trans. Nucl. Sci. NS-26, 3842 (1979).

7. J.S. Schuchman, J.B. Godel, W. Joran, T. Oversluizen, J. Vac. Sci. & Technology 16, No. 2 (1979).

8. J. Galayda, R. N. Heese, H.C.H. Hsieh, H. Kapfer, "The NSLS Magnet System," IEEE Trans. Nucl. Sci. NS-26, 3919 (1979).

9. K. Batchelor, B. Culwick, J. Goldstick, J. Sheehan, J. Smith, "Distributed Control System for the NSLS," IEEE Trans. Nucl. Sci. NS-26, 3387 (1979).

10. K. Batchelor, J. Galayda, R. Hawrylak, IEEE Trans. Nucl. Sci. NS-28, No. 3, 2839 (1981).

11. T. Dickinson, R. Rheaume, IEEE Trans. Nucl. Sci. NS-28, No. 3, 2997 (1981).

12. K.W. Robinson, CEA Report 14 (1956).

13. H. Winick, R. Helm, Nucl. Instr. Methods 152 (1978) 9.

14. H. Hsieh, S. Krinsky, A. Luccio, A. van Steenbergen, IEEE Trans. Nucl. Sci. NS-28, 3, (1981) 3292.

15. K. Halbach, private communication.

16. K. Halbach, J. Chin, E. Hoyer, (LBL); H. Winick, R. Cronin, J. Young, Y. Zambre, (SSRL), IEEE Trans. Nucl. Sci. NS-28, 3, (1981) 3136.

17. H. Motz, J. Appl. Phys. 22 (1951) 527.

18. J. Hastings, D. Moncton, private communication.

19. D. Alferov, Yu. Baskmakov, G. Bessonov, Sov. Phys. Tech. Phys. 18 (1974) 1336.

20. S. Krinsky, Nucl. Instr. & Methods 172 (980) 73.

21. A. N. Didenko, JETP 49(6) (1979) 973.

22. J. Schwinger, Phys. Rev. 75 (1949) 1912.

23. D. Ivanenko, A. Sokolov, Doklady Akad Nauk (SSSR) 59 (1948) 1551.

24. European Synchrotron Radiation Facility Design Report, Suppl. III, p. 18; B. Buras, G. Marr, editors.

25. R. Coisson, S. Guiducci, M. Preger, "Multipole Wigglers as Sources of Synchrotron Radiation," to be published in Nucl. Instr. & Methods.

26. M. Howells, private communication.

27. C. Pellegrini, IEEE Trans. Nucl. Sci. NS-26 (1979) 3791.

28. L. R. Elias, W. Fairbanks, J. Madey, H. Schwettman, T. Smith, Phys. Rev. Letters 36 (1976) 717.

29. J. Blewett, L. Blumberg, A. Campillo, R. di Nardo, H. Hsieh, S. Krinsky, A. Luccio, C. Pellegrini, J. Schuchman, P. Takacs, A. van Steenbergen, IEEE Trans. Nucl. Sci. NS-28, 3, (1981)

30. A. Renieri, Trans. Nucl. Sci. NS-26 (1979) 3791.

31. A. Sandorfi, M. Levine, "A proposal for a high energy gamma ray beam for medium energy nuclear physics at the National Synchrotron Light Source," Spring, 1982.

32. L. Federici, et al. Letters Nuovo Cimento 27 (1980) 389.

33. A. Sandorfi, private communication.

Fig. 1. NSLS INJECTOR

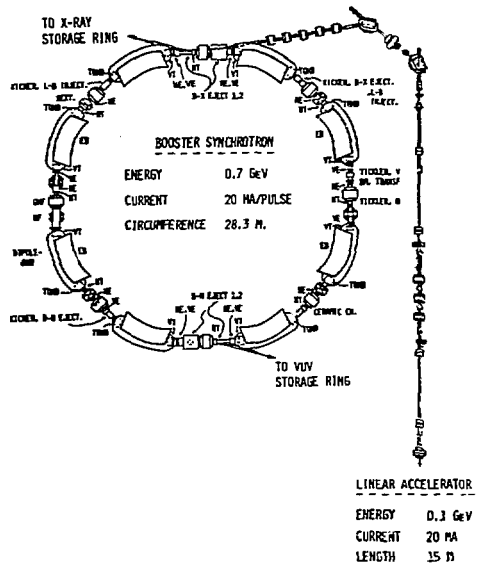

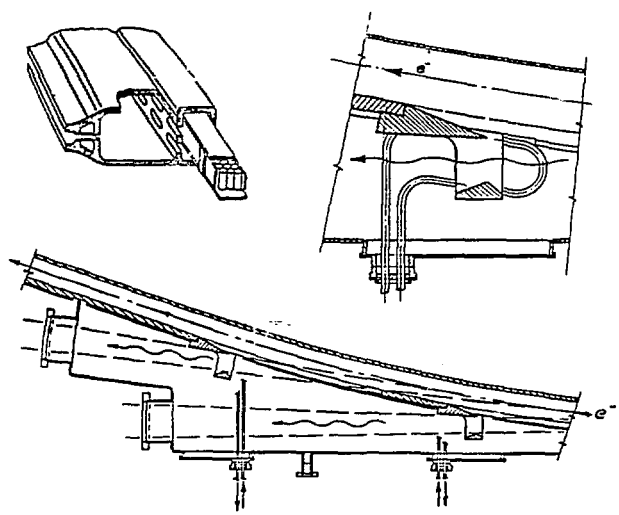

Fig. 6. NSLS, X-RAY VACUUM CHAMBER

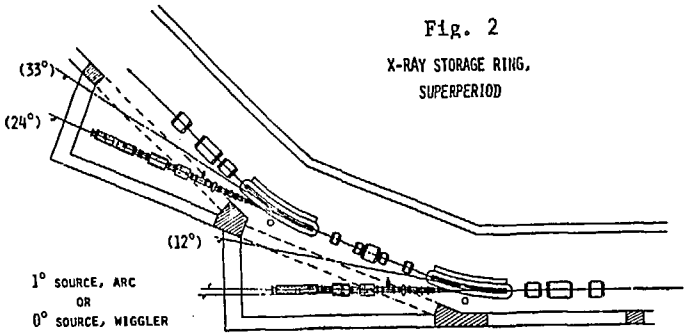

Fig. 2

X-RAY STORAGE RING,
SUPERPERIOD

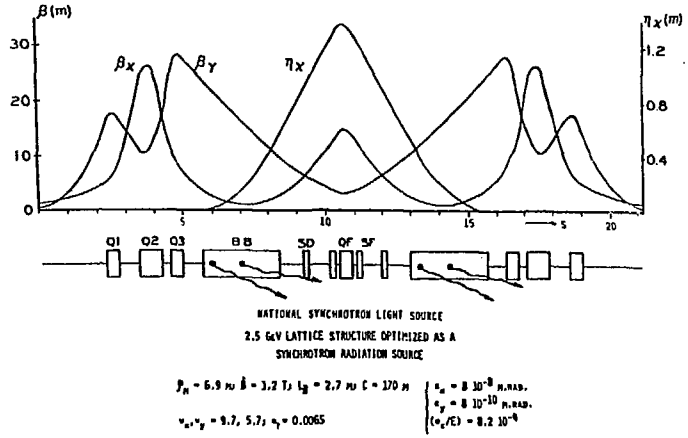

Fig. 3

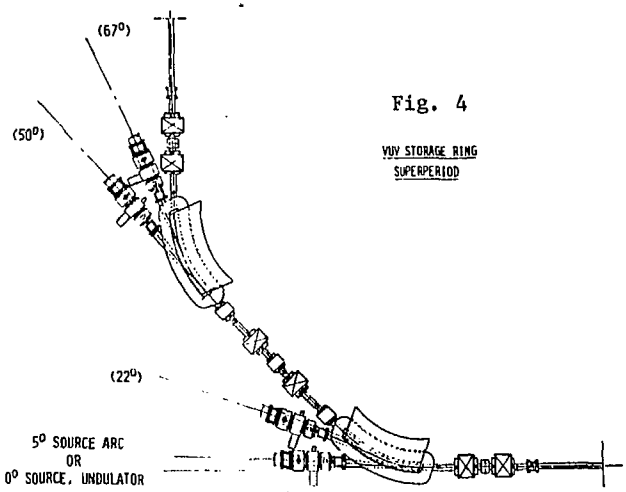

Fig. 4

VUV STORAGE RING
SUPERPERIOD

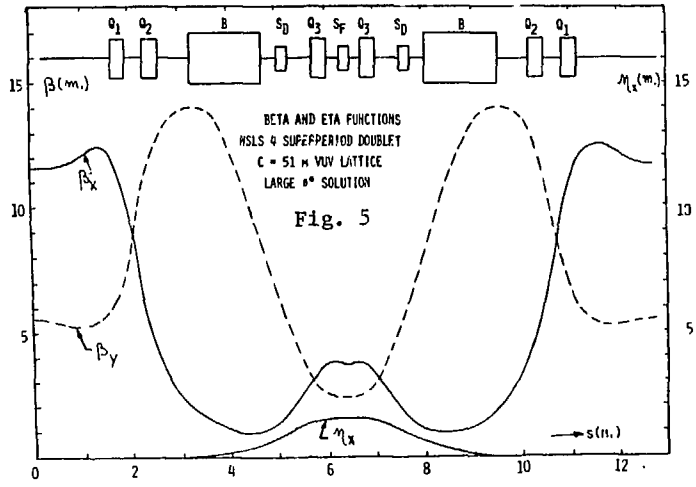

Fig. 5

Fig. 7. NSLS SUPERCONDUCTING WIGGLER

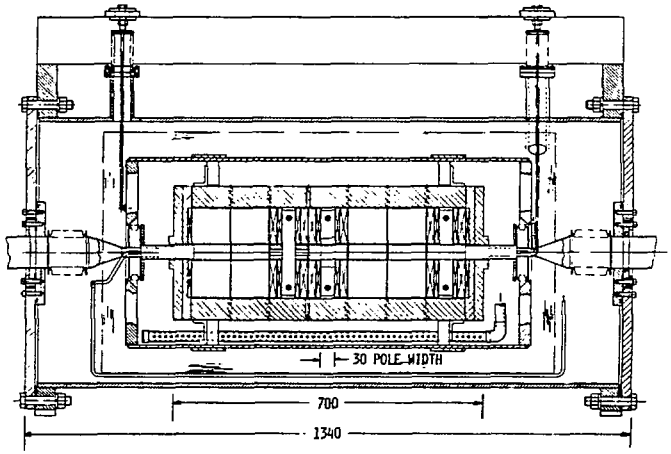

Fig. 8. PERMANENT MAGNET UNDULATOR

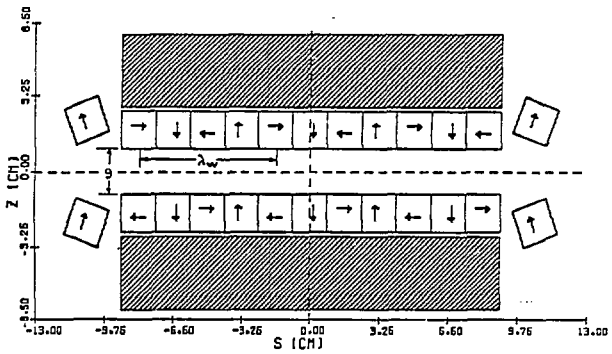

$K = 0.9\, B\, \lambda_w$; $B = \text{CONST.}\ B_c \exp(-\pi g/\lambda_w) \cdot F\ (\text{GEOMETRY})$

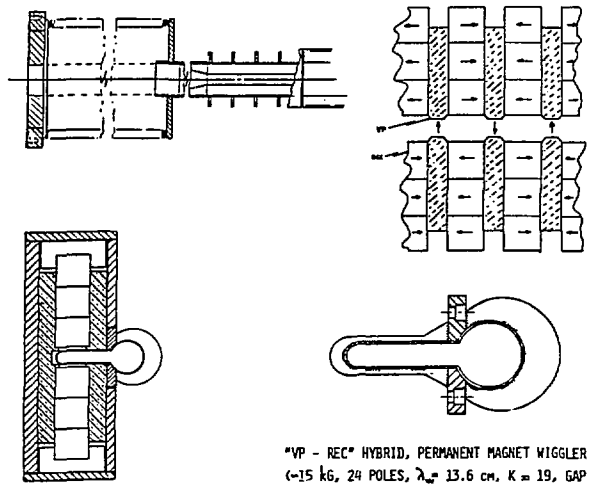

"VP - REC" HYBRID, PERMANENT MAGNET WIGGLER
(~15 kG, 24 POLES, λ_w = 13.6 cm, K = 19, GAP = 2 cm)

Fig. 9

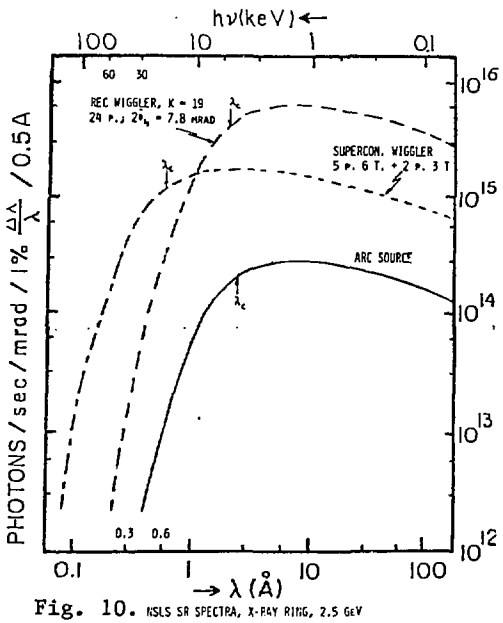

Fig. 10. NSLS SR SPECTRA, X-RAY RING, 2.5 GeV

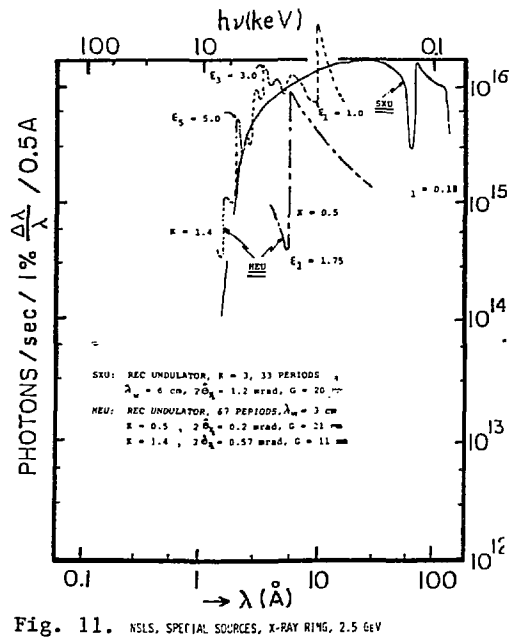

Fig. 11. NSLS, SPECTAL SOURCES, X-RAY RING, 2.5 GeV

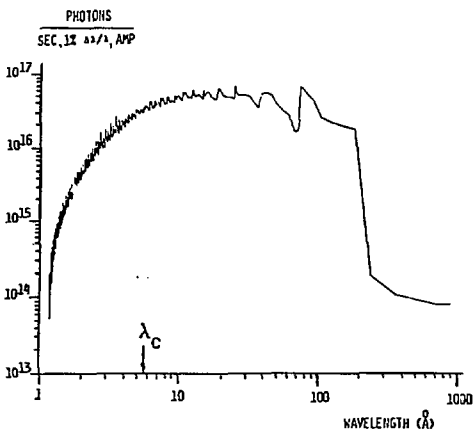

Fig. 12. NSLS UNDULATOR SPECTRUM, X-RAY, 2.5 GeV
(K = 3, 40 PERIODS, λ_w = 6 cm, $2\theta_x$ = 1.2 MRAD, G = 20 MM, γ = 3.0)

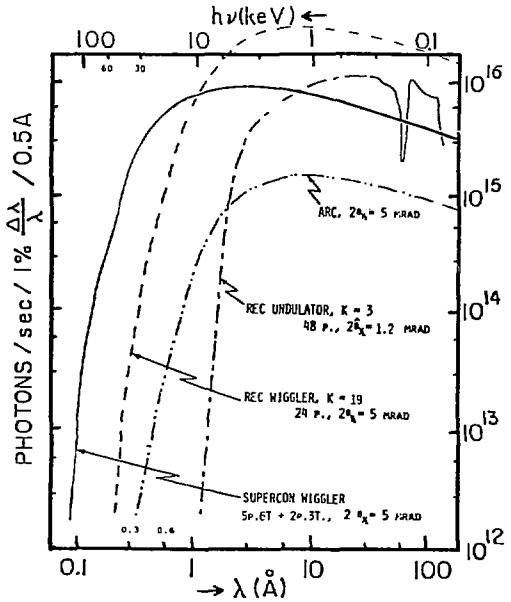

Fig. 13. NSLS, SPECIAL SOURCES, X-RAY RING, 2.5 GeV

Fig. 14. UNDULATOR STRUCTURE FOR THE FEL
(PERM. MAGNETS, λ_0 = 6.5 cm, B_0 = 0.1 - 0.6 T., N = 39)

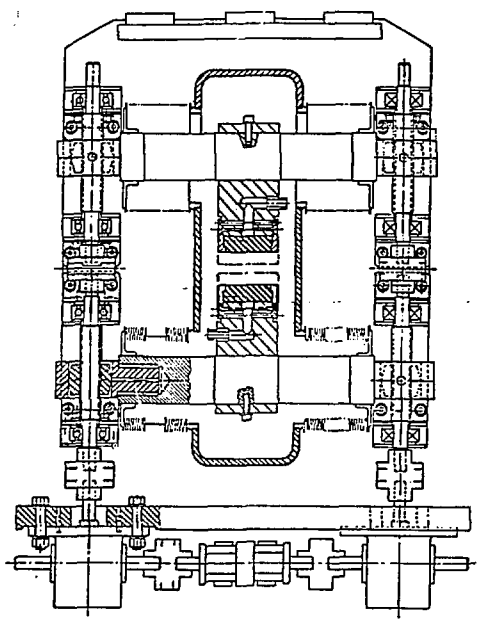

N=38, λ_w=6.5 cm; K=1.0; γ=1370; θ_x=0.5

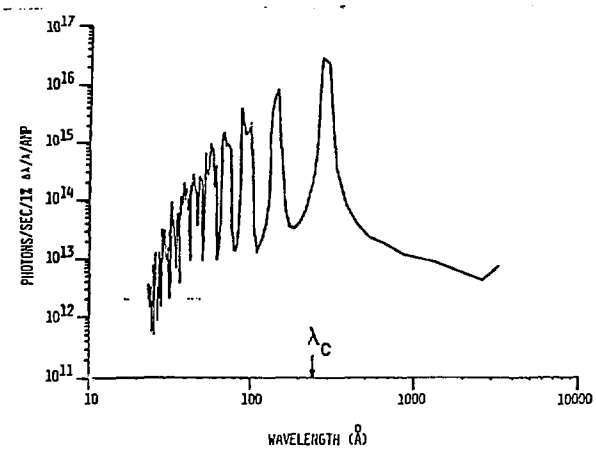

Fig. 15. NSLS UNDULATOR (K = 1) SPECTRUM, VUV RING

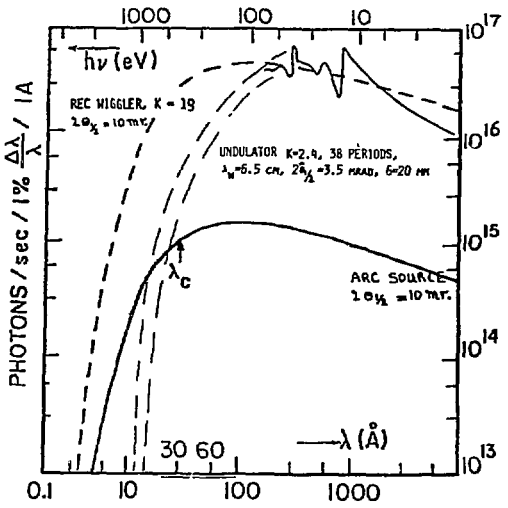

Fig. 16. NSLS SPECTRUM, VUV, 0.7 GeV

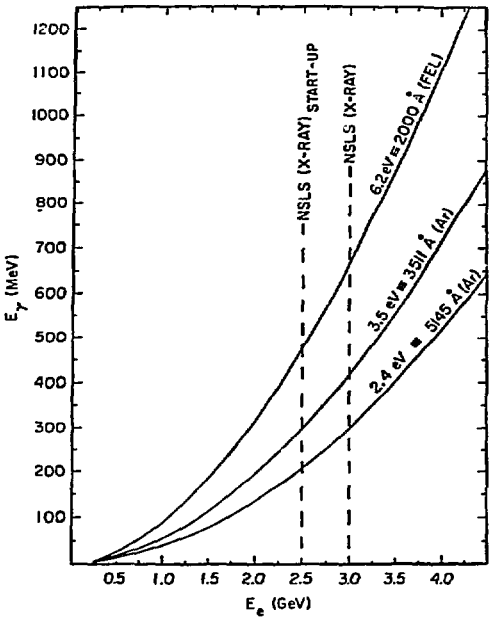

Fig. 18. ENERGY RANGE, BACKSCATTERED γ SOURCE

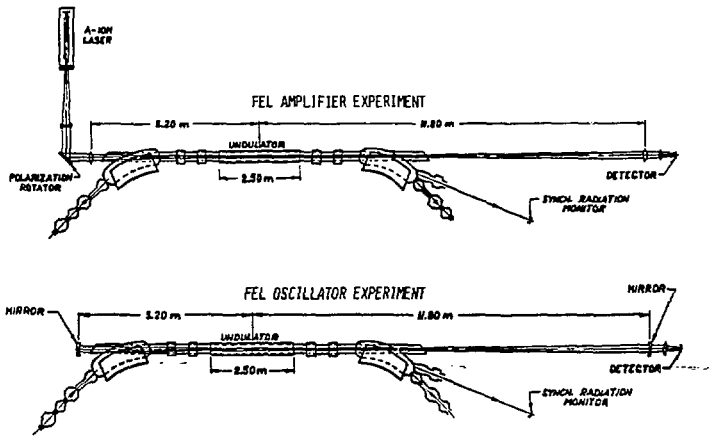

Fig. 17. NSLS FEL EXPERIMENT

Fig. 19. COMPTON BACKSCATTERED X SOURCE DEVELOPMENT

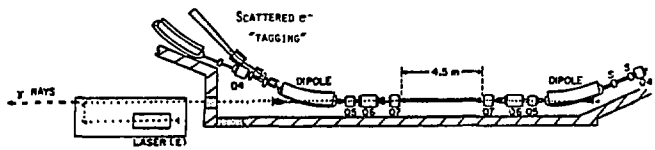

e⁻ BEAM: E = 2.5 GeV
I = 0.5A
N = 1.8 10^{12}

ℰ BEAM: ℰ = 3 eV
P = 5 W
N = 3 10^{11} Ph./Int.Vol.

X BEAM: ℰ = 255 KeV
*ΔE = 2.7 KeV FOR ALL E_γ
I ≈ 10^7/sec
P ≥ 90%
*WITH e⁻ TAGGING

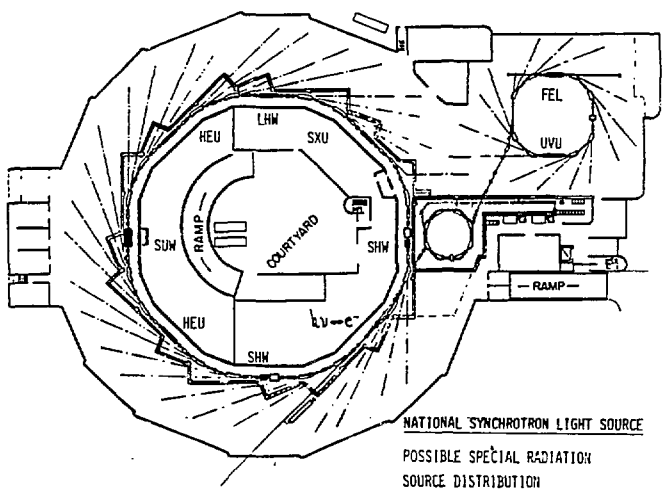

NATIONAL SYNCHROTRON LIGHT SOURCE

POSSIBLE SPECIAL RADIATION
SOURCE DISTRIBUTION

Fig. 20